Dependence of electric energy output from a lead zirconate titanate ceramic piezoelectric element on impact conditions

ARTICLE *in* MATERIALS CHEMISTRY AND PHYSICS · JULY 2011

Impact Factor: 2.26 · DOI: 10.1016/j.matchemphys.2011.02.050

Junhui Hu
Nanjing University of Aeronautics & Astron…

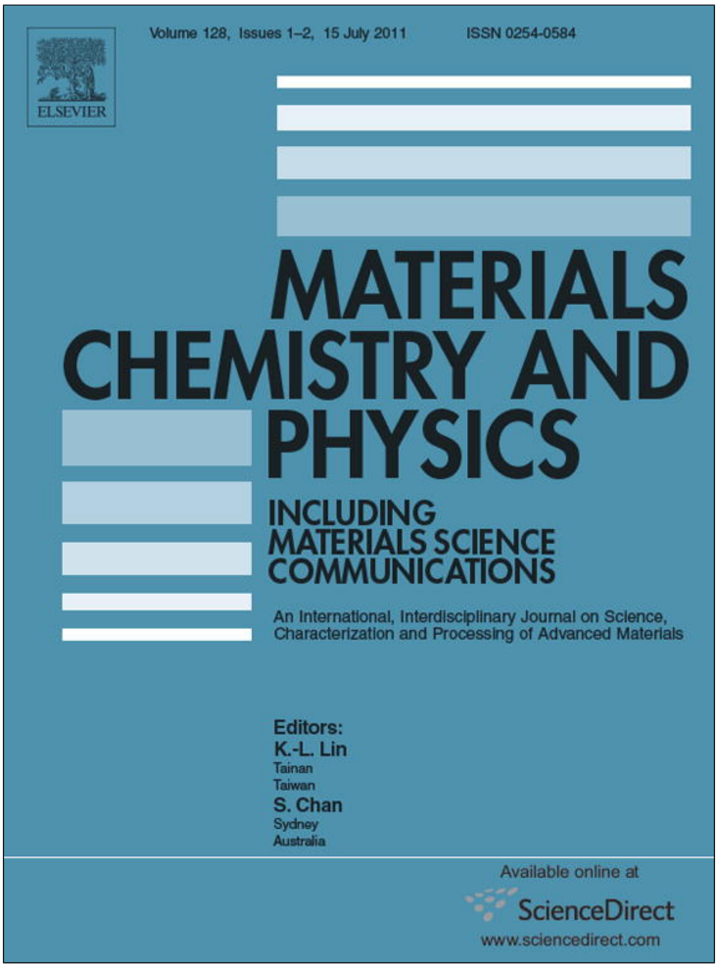
Volume 128, Issues 1–2, 15 July 2011
ISSN 0254-0584
ELSEVIER
MATERIALS CHEMISTRY AND PHYSICS
INCLUDING MATERIALS SCIENCE COMMUNICATIONS
An International, Interdisciplinary Journal on Science, Characterization and Processing of Advanced Materials
Editors:
K.-L. Lin
Tainan
Taiwan
S. Chan
Sydney
Australia
Available online at
ScienceDirect
www.sciencedirect.com

Materials Chemistry and Physics 128 (2011) 172–176

Contents lists available at ScienceDirect

Materials Chemistry and Physics

journal homepage: www.elsevier.com/locate/matchemphys

Dependence of electric energy output from a lead zirconate titanate ceramic piezoelectric element on impact conditions

Junhui Hu[a,*], Nelson Tjiu[b]

[a] *Precision Driving Lab, Nanjing University of Aeronautics and Astronautics, Yudao Street 29, Nanjing 210026, China*
[b] *School of Electrical and Electronic Engineering, Nanyang Technological University, 639798, Singapore*

ARTICLE INFO

Article history:
Received 9 November 2010
Received in revised form 8 February 2011
Accepted 23 February 2011

Keywords:
Piezoelectric element
Impact conditions
Generators
Electric energy

ABSTRACT

In this work, dependence of electric energy output of impacted piezoelectric element on impact conditions is experimentally investigated. Investigated impact parameters include impact position, radius of impact sphere, orientation of the hitting object, and material and configuration of the buffer layer. It is found that the electric energy output of impacted piezoelectric plate may be increased by impacting the buffer layer at its center, decreasing the contact area between the hitting object and buffer layer, reducing internal energy absorption in the mechanical buffer layer and avoiding wave reflection in the buffer layer. The experimental phenomena are theoretically explained and analyzed, based on the piezoelectric constitutive equation and Hertz's impact theory.

1. Introduction

The piezoelectric generator, which uses piezoelectricity of piezoelectric components to convert mechanical vibration into electric energy, has potential applications in wireless electronics, low-power portable electronic devices and ubiquitous computing systems. Electric output power of piezoelectric generator can reach up to several hundred milli-watts. Various structures of piezoelectric generators have been proposed and researched [1–12], and some of them are based on the impact between a hitting object and piezoelectric component [13,14]. In the piezoelectric generator using impact mode, piezoelectric components are bonded under a mechanical buffer layer, and the mechanical buffer layer is hit by solid object with kinetic energy. The impact causes vibration in the buffer layer and piezoelectric component, which results in an AC output voltage across the two electrodes of the piezoelectric component. The buffer layer is used to make impact stress in the piezoelectric component uniform, which prevents the piezoelectric component from breaking into pieces.

So far the research on effects of impact conditions of piezoelectric generator on its electric energy output is scarce. This is hindering the improvement and optimal design of the impact mode based piezoelectric generator. In [14], authors proposed to use the Hertz's impact model [15] to analyze the operation of a piezoelectric generator working in impact mode. However, detailed analyses were not carried out.

In this work, we have experimentally investigated the dependence of electric energy output of impacted piezoelectric plate on impact conditions. Impact parameters investigated by this work include impact position, radius of impact sphere, orientation of the hitting object, and material and configuration of the buffer layer. Observed experimental phenomena not only provide guidelines for the optimal design of impact mode based piezoelectric generators, but also give out the direction for further theoretical research of the piezoelectric generators.

2. Experimental design and setup

Fig. 1 shows the experimental setup for investigating the effects of impact conditions on electric energy output of piezoelectric element. A piezoelectric disk (Fuji Ceramics, C203) with a diameter of 26 mm and thickness of 1 mm is placed on a plastic stage. Metal buffer layer is bonded on the top surface of the piezoelectric disk. A hitting object released above the metal buffer layer falls off and hits the buffer layer. AC output voltage generated by the piezoelectric disk is applied to an electrolytic capacitor of $C = 33\ \mu F$ via a full wave rectifier (36MB-A). Before each impact, the capacitor is short circuited. Measuring the DC voltage V_c across the capacitor after each impact, electric energy generated by each impact can be calculated out by

$$E = 0.5CV_c^2 \tag{1}$$

The piezoelectric disk is poled in the thickness direction, as indicated in Fig. 1(a). Its electromechanical coupling factor k_t is 0.49; dielectric constant $\varepsilon_{33}^T/\varepsilon_0$ is 1450; piezoelectric charge constant d_{33} is 325×10^{-12} C N^{-1}; piezoelectric charge constant d_{31} is -145×10^{-12} C N^{-1}; piezoelectric voltage constant g_{33} is 25.6×10^{-3} V m N^{-1}; piezoelectric voltage constant g_{31} is -11.2×10^{-3} V m N^{-1}; Young's modulus Y_{33}^E is 6.0×10^{10} N m^{-2}; Poisson's ratio is 0.29; mechanical quality factor Q is 2000; dissipate factor is 0.3; density is 7700 kg m^{-3}. Circular disks made of stainless steel, aluminum, brass and copper are used as the buffer layer. Their diameter is 26 mm, and their mass and thickness are shown in Table 1. The shape of stainless steel hitting objects used in experiments includes sphere, cone and cylinder, as shown in

* Corresponding author.
E-mail addresses: ejhhu@nuaa.edu.cn, ejhhu@ntu.edu.sg (J. Hu).

0254-0584/$ – see front matter © 2011 Elsevier B.V. All rights reserved.
doi:10.1016/j.matchemphys.2011.02.050

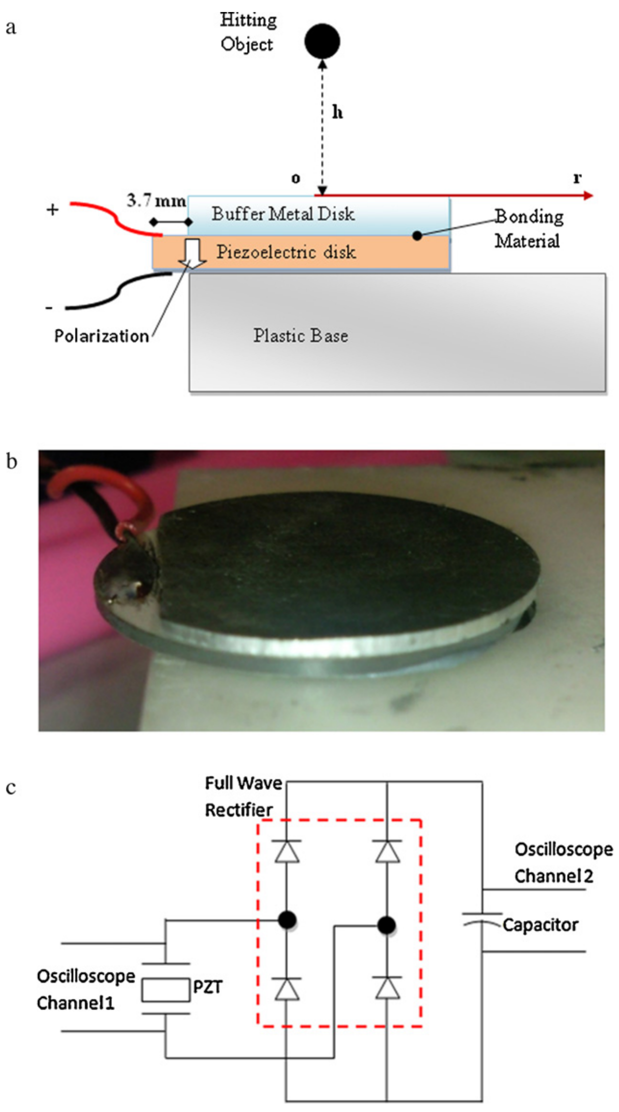

Fig. 1. Experimental setup to investigate the effects of the impact structure of piezoelectric generator on its output energy. (a) Schematic drawing of mechanical part of experimental setup. (b) Image of mechanical part of experimental setup. (c) Circuit for measuring the electric energy output per impact.

Table 1
The dimensions and mass of the buffer disks.

Buffer disks	Mass (g)	Diameter (mm)	Height/thickness(mm)
Steel	4.07 (BDS1)	26	1
	7.62 (BDS2)	26	2
	11.93 (BDS3)	26	3
Aluminum	1.37	26	1
Brass	4.60	26	1
Copper	4.69	26	1

Table 2
The dimensions and mass of the hitting objects.

Hitting objects[a]	Mass (g)	Diameter (mm)	Thickness/height (mm)
Sphere 1	2.04	8	–
Sphere 2	16.72	16.67	–
Sphere 3	28.20	19.05	–
Sphere 4	54.93	23.81	–
Sphere 5	66.76	25.4	–
Cube	2.05	6.43	6.43
Cone	4.84	10	23
Cylinder	14.12	10	23

[a] All of the hitting objects in this table are made of stainless steel.

Fig. 2, and their mass and size are shown in Table 2. The spherical stainless steel hitting object has five diameters from 8 mm to 25.4 mm. The experiments are carried out in air, and the initial speed of hitting object is zero.

In the experiments, unless otherwise specified, the initial height of hitting object h is 100 mm; the hitting point is at the center of buffer layer; buffer layer BDS1 (see Table 1) is bonded onto piezoelectric disk by adhesive material Epoxy Fix – Super Steel (Selleys) with a thickness of 0.1 mm; stainless steel sphere with a diameter of 8 mm is used as the hitting object.

3. Results and discussion

The effect of impact position on the electric energy output per impact was measured for two different thicknesses (0.1 mm and 1 mm) of adhesive layer, and the results are shown in Fig. 3. It is seen that when the sphere hits the center of buffer disk, the electric energy output is maximum; as impact location shifts to the side of buffer disk, the electric energy output decreases. Uniformity of impact induced stress in the buffer layer depends on the impact location. As impact location shifts from the center to the side of buffer layer, spatial non-uniformity of impact induced stress in the buffer layer increases, which results in the decrease of electric energy output. It is also seen that the structure with thinner adhesive layer has larger electric energy output. This is because in thicker bonding layer there is more energy absorption.

The effect of the radius of stainless steel hitting sphere on the electric energy output per impact was measured for different initial heights of hitting sphere, and the result is shown in Fig. 4. It is seen that as the diameter of hitting sphere increases, the electric energy output per impact increases; when the diameter of hitting sphere is larger than some critical value (23.8 mm), the electric output power per impact decreases as the diameter increases. The former phenomenon is caused by the increase of impact momentum of the hitting sphere, and the latter may be caused by the increase of contact area between the hitting sphere and buffer layer. The speed of hitting object relative to the buffer layer is

$$v = \sqrt{2gh} \tag{2}$$

The impact force F is

$$F \propto \frac{mv}{\Delta t} \tag{3}$$

where m is the mass of hitting object, Δt is the impact time and mv is the impact momentum. The open-circuit electric field E in the piezoelectric disk is

$$E = -g_{33}\frac{F}{A} \propto \frac{g_{33}mv}{\Delta tA} \tag{4}$$

where A is the contact area between the hitting object and buffer layer.

Mass m of the hitting sphere, contact area A between the hitting object and buffer layer, and impact time Δt increase with the increase of the diameter of hitting sphere. When the diameter of hitting sphere is less than the critical value (23.8 mm), increase of m is faster than that of ΔtA as the diameter increases, which causes the increase of electric energy output with the increase of diameter. When the diameter of hitting sphere is greater than the critical value, increase of m is slower than that of ΔtA as the diameter increases, which causes the decrease of electric energy output with the increase of diameter.

Fig. 5 shows the electric energy output per impact versus impact position for a stainless hitting sphere (sphere 1) and cube with the same mass of 2 g. The diameter of sphere is 8 mm, and side length of cube is 6.43 mm, as shown in Table 2. In the experiment, the distance between the lower end of the hitting objects and buffer layer is 100 mm, and the bottom surface of cube at the initial position is parallel to the buffer layer. The figure shows that for the same impact momentum, the shape of impact part of the hitting objects

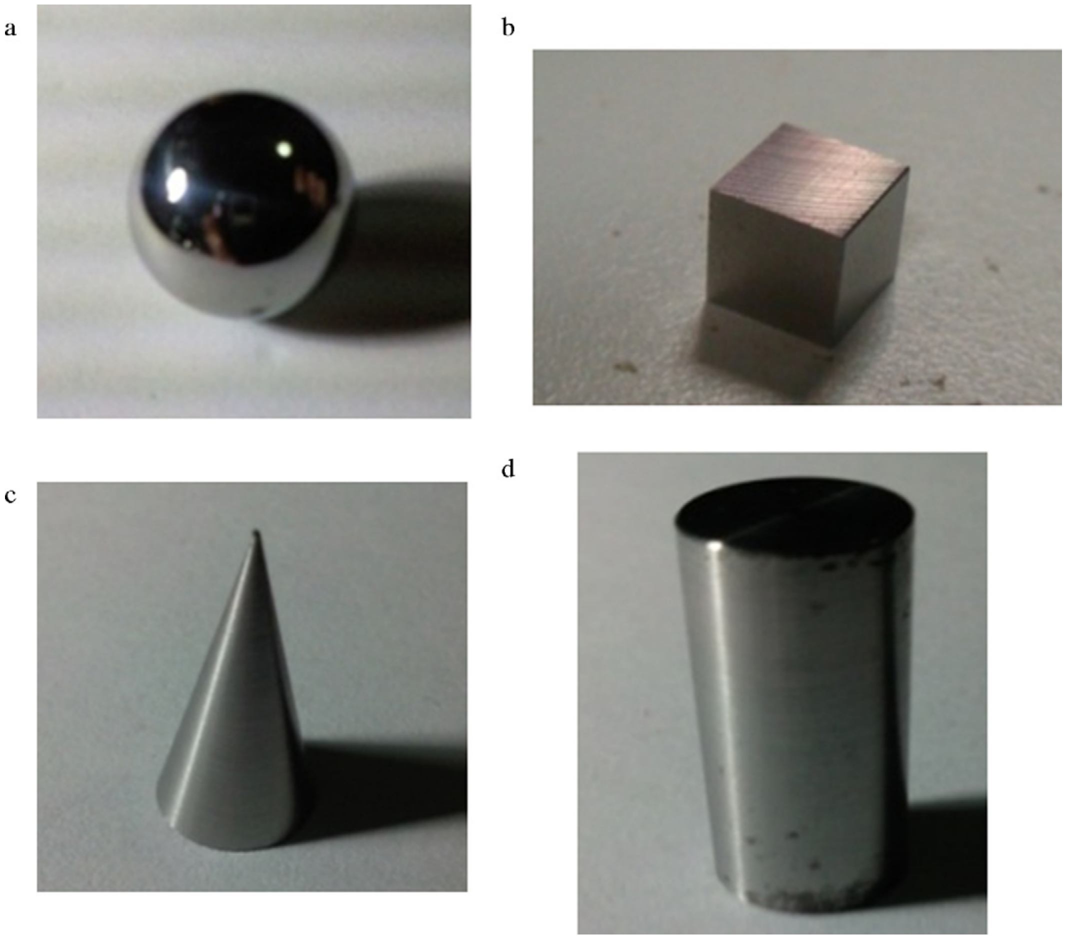

Fig. 2. Hitting objects used in experiments. (a) Stainless ball. (b) Stainless cube. (c) Stainless cone. (d) Stainless cylinder.

affects the electric energy output, and the sphere has larger electric energy output than cube. The contact area between the sphere and buffer layer is less than that between the cube and buffer layer. This causes a larger open-circuit electric field in the piezoelectric component hit by the sphere (see Eq. (4)).

Fig. 6 shows the electric energy output per impact when the buffer layer is hit by a stainless cone with the mass of 4.84 g initially at different heights (h). The cone is 23 mm high and its bottom diameter is 10 mm. Two impact patterns are used in experiments, i.e. pattern A and pattern B. In pattern A, the sharp end of cone is used to hit the buffer layer. In pattern B, the bottom face of cone used to hit the buffer layer. At given h, patterns A and B have the same impact speed and momentum. The difference of electric energy output per impact between patterns A and B indicates that the impact area between the hitting object and buffer layer does affect the electric energy output. Smaller impact area causes larger electric energy output.

A similar experiment has been carried out for a stainless cylinder initially at different heights (h), as shown in Fig. 7(a), and the result is shown in Fig. 7(b). The cylinder has mass of 14.12 g, diameter of 10 mm and height of 23 mm. Two impact patterns are used in experiments, i.e. pattern A and pattern B. In pattern A, the side of cylinder is used to hit the buffer layer. In pattern B, the end surface

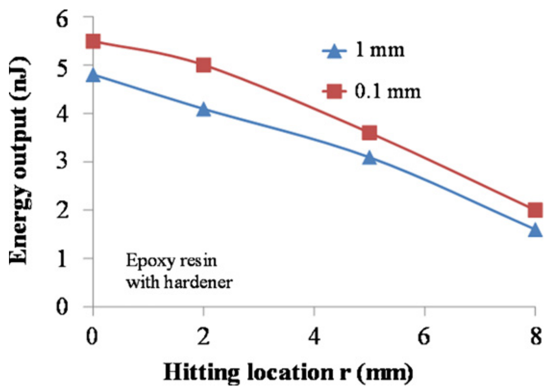

Fig. 3. Electric energy output per impact versus hitting location for two adhesive layers with thickness of 0.1 mm and 1 mm, respectively.

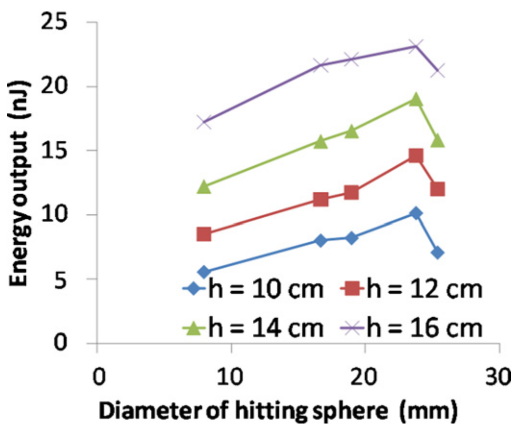

Fig. 4. Effect of the diameter of stainless steel hitting sphere on the electric energy output per impact. The hitting point is at $r = 0$.

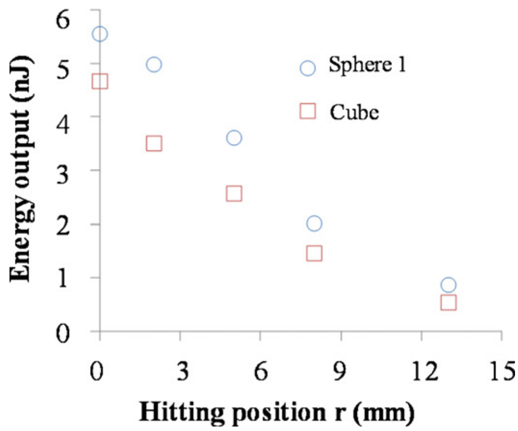

Fig. 5. Comparison of electric energy output between the impacts of sphere-buffer disk and cube-buffer disk. The sphere and cube have the same mass of 2 g, and are made of stainless steel. The buffer disk (BDS1 in Table 2) is 1 mm thick. The calculated impact speed of the two impacts is 1.4 m s^{-1}. The hitting point is at $r = 0$.

is used to hit the buffer layer. From Fig. 7(b), it is seen that pattern A has larger electric energy output per impact than pattern B, which also indicates that smaller impact area causes larger electric energy output.

To investigate the effect of material and configuration of the buffer layer on the electric energy output per impact, experimental setup shown in Fig. 8 is used. Buffer disks X and Y are aligned with their center and bonded by Epoxy Fix – Super Steel (Selleys) with a thickness of 0.1 mm. The diameter and thickness of each buffer disk is 26 mm and 1 mm, respectively. Aluminum, brass and copper are used as the material of buffer disk. The buffer layer is bonded onto the piezoelectric disk by Epoxy Fix – Super Steel (Selleys) with a

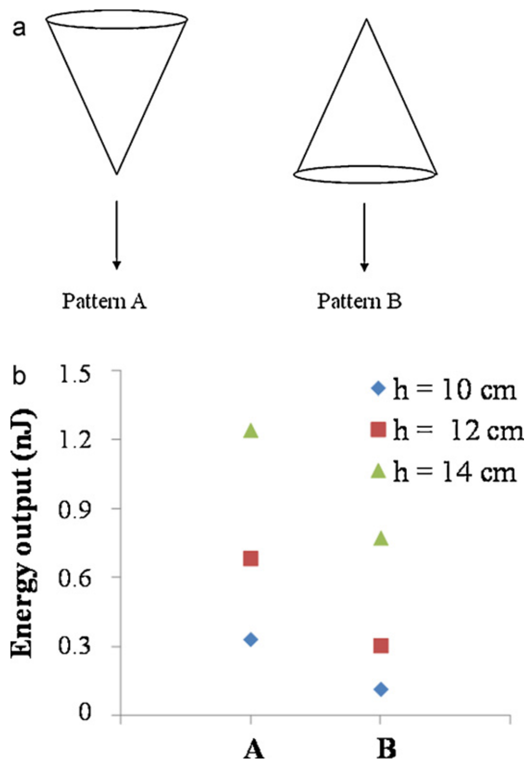

Fig. 6. Electric energy output per impact between a cone and buffer disk. (a) Two different impact orientations. (b) Comparison of electric energy output of the two impact orientations. The cone is made of stainless steel, and its mass and dimension are shown in Table 1. The buffer disk (BDS1) is also made of stainless steel, and its mass and dimensions are shown in Table 2. The hitting point is at $r = 0$.

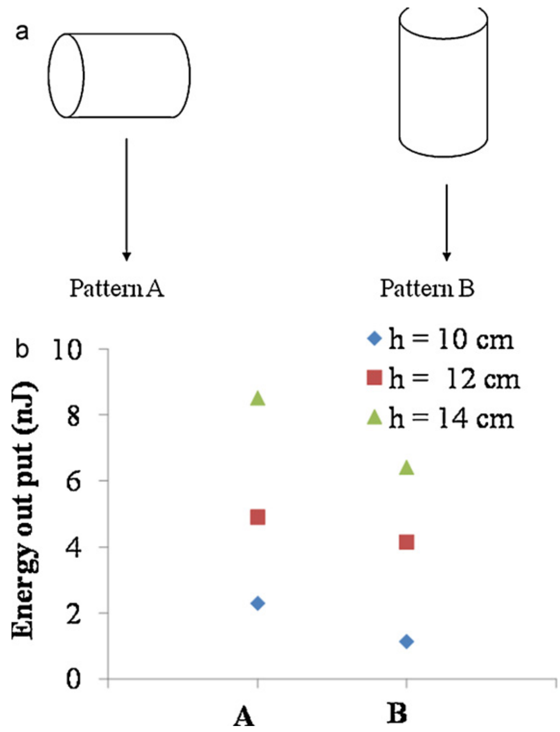

Fig. 7. Electric energy output per impact between a cylinder and buffer disk. (a) Two different impact orientations. (b) Comparison of electric energy output per impact. The cylinder is made of stainless steel, and its mass and dimension are shown in Table 1. The buffer disk (BDS1) is also made of stainless steel, and its dimensions and mass are shown in Table 2. The hitting point is at $r = 0$.

thickness of 0.1 mm. Sphere 1 in Table 2 is used as the hitting object, and the impact is at the center of buffer layer. The initial height h of hitting sphere is 100 mm. Measured electric energy output per impact for different materials and configurations is shown in Fig. 9. In the figure, AA, BB, CC, AB, BA, AC, CA, BC and CB represent material and configuration of the buffer layer. The first letter in them represents material of buffer disk X and the second one represents material of buffer disk Y, that is, the A represents aluminum; the B represents brass; the C represents copper.

From Fig. 9, the following phenomena are observed. (a) Metal material of the buffer layer has effect on the electric energy output, and BB and CC have larger electric energy output than AA; (b) using

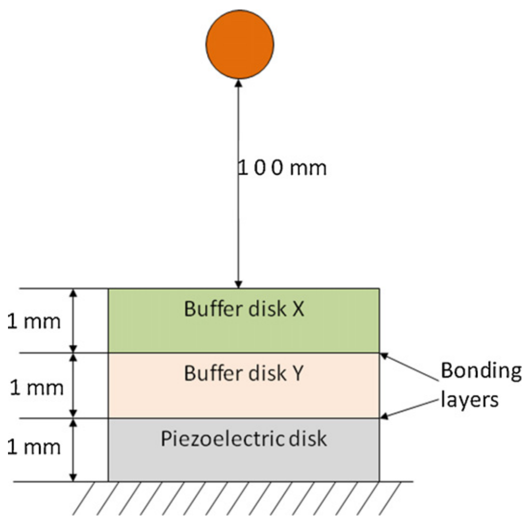

Fig. 8. Experimental set up to investigate the effect of material and configuration of buffer disk on electric energy output.

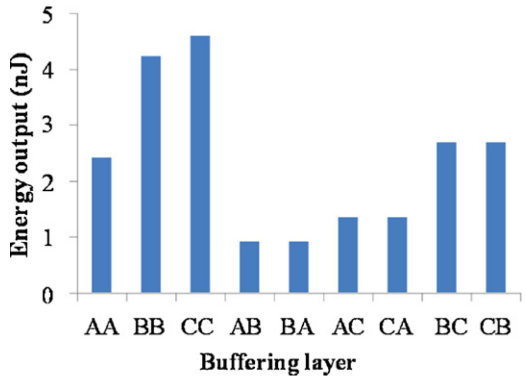

Fig. 9. Electric energy output for different buffer layers. Sphere 1 is used in the experiment with $r = 0$ and $h = 10$ cm.

single metal material in the buffer layer causes larger output energy than using two different metal materials; and (c) when two different metal materials are used, the spatial sequence of the materials has little effect on the electric energy output, for example, AB and BA have very close electric energy output per impact and so have buffer layers AC and CA.

The impact time Δt between the hitting sphere and buffer layer can be estimated by the Hertz's impact theory [15]. Assuming the radius and mass of the buffer layer to be infinite, we have

$$\Delta t = \frac{2.87m^{0.4}}{v^{0.2}R^{0.2}}D \tag{5}$$

$$D = \left(\frac{1}{\rho c^2} + \frac{1}{\rho_x c_x^2}\right)^{0.4} \tag{6}$$

in which R is the radius of the hitting sphere, ρ and ρ_x are the density of the hitting sphere and top buffer disk X, respectively, c and c_x are the sound speed in the hitting sphere and top buffer disk X, respectively. In the experiment shown in Fig. 8, m, v and R are constant, so the impact time Δt only depends on parameter D. D values for the impact between stainless steel and aluminum, between stainless steel and brass, and between stainless steel and copper are calculated, and results are as follows: $D = 0.011$ for the impact between stainless steel and aluminum; $D = 0.0095$ for the impact between stainless steel and brass; $D = 0.0087$ for the impact between stainless steel and copper. In the calculation, the density of and sound speed in aluminum are 2700 kg m^{-3} and 6300 m s^{-1}, respectively; the density of and sound speed in brass are 8500 kg m^{-3} and 4700 m s^{-1}, respectively; the density of and sound speed in copper are 8900 kg m^{-3} and 5000 m s^{-1}, respectively; the density of and sound speed in stainless steel are 7700 kg m^{-3} and 6100 m s^{-1}, respectively. The calculated D values have little difference for the impacts, which means the impact time has little change in the experiment shown in Fig. 8.

In the experiment shown in Fig. 8, AA, BB and CC have the same adhesive layers, dimensions of buffer layer, impact speed and momentum, and very close theoretical impact time. Also, the loss factor of aluminum is the smallest of those of aluminum (0.3×10^{-5} to 10×10^{-5}), brass (0.2×10^{-3} to 1×10^{-3}) and copper (2×10^{-3}). So phenomenon (a), given in Fig. 9, is believed to be caused by different deformations of the surface of buffer layer. Among the aluminum, brass and copper buffering layers, the surface of aluminum buffering layer is the easiest one to deform because the bulk modulus of aluminum (75 GPa) is less than those of brass (136 GPa) and copper (160 GPa), and Young's modulus of aluminum (73 GPa) is less than those of brass (100 GPa) and copper (120 GPa). So energy absorbed by the surface of aluminum buffering layer is the largest for the same impact conditions. Phenomenon (b) shown in Fig. 9, may be caused by the wave reflection at the internal interface between buffer disks X and Y. When buffer disks X and Y are made of different materials, the reflection at the interface increases and more energy cannot be transmitted to the piezoelectric component.

4. Summary

We have experimentally investigated the effects of the impact conditions on electric energy output of an impacted piezoelectric disk. It is found that the impact location, radius of curvature of hitting object, orientation and shape of hitting object, and material and configuration of the buffer layer affect the electric energy output per impact. It is experimentally found that the electric energy output may be increased by impacting the buffer layer at its center, decreasing the contact area between the hitting object and buffer layer, reducing the internal energy absorption in the buffer layer and avoiding wave reflection in the buffer layer. The results obtained in this work provide guidelines for the optimization of piezoelectric generators based on impact mode.

References

[1] J. Kymissis, C. Kendall, J. Paradiso, N. Gershenfeld, Proc. 2nd IEEE Int. Conf. Wearable Computing, California, 1998, pp. 132–139.
[2] H. Li, A. Lal, J. Blanchard, D. Henderson, J. Appl. Phys. 92 (2002) 1122.
[3] C. Keawboonchuay, T.G. Engel, IEEE Trans. Ultrason. Ferroelect. Freq. Control 50 (10) (2003) 1377.
[4] S. Roundy, P.K. Wright, Smart Mater. Struct. 13 (2004) 1131.
[5] H.W. Kim, A. Batra, S. Priya, K. Uchino, D. Markley, R.E. Newnham, H.F. Hofmann, Jpn. J. Appl. Phys. 43 (2004) 6178.
[6] J. Yang, H. Zhou, Y. Hu, Q. Jiang, IEEE Trans. Ultrason. Ferroelect. Freq. Control 52 (2005) 1872.
[7] D. Guyomar, A. Badel, E. Lefeuvre, C. Richard, IEEE Trans. Ultrason. Ferroelect. Freq. Control 52 (4) (2005) 584.
[8] S. Kim, W.W. Clark, Q.M. Wang, J. Intell. Mater. Syst. Struct. 16 (2005) 853.
[9] S.P. Beeby, M.J. Tudor, N.M. White, Meas. Sci. Technol. 17 (2006) 175 (R).
[10] S.R. Anton, H.A. Sodano, Smart Mater. Struct. 16 (2007) R1.
[11] H.P. Hu, H. Xue, Y.T. Hu, IEEE Trans. Ultrason. Ferroelect. Freq. Control 54 (6) (2007) 1177.
[12] K.A. Cook-Chennault, N. Thambi, A.M. Sastry, Smart Mater. Struct. 17 (2008) 043001.
[13] M. Umeda, K. Nakamura, S. Ueha, Jpn. J. Appl. Phys. (Part I) 35 (5B) (1996) 3267.
[14] J. Hu, J. Jong, C. Zhao, IEEE Trans. Ultrason. Ferroelect. Freq. Control 57 (2) (2010) 386.
[15] A.E.H. Love, A Treatise on the Mathematical Theory of Elasticity, Dover Publications, New York, NY, 1944, p. 198.